AIAA JOURNAL
Vol. 32, No. 9, September 1994

Passive Spatial Confinement of Impulsive Responses in Coupled Nonlinear Beams

Alexander F. Vakakis*
University of Illinois, Urbana, Illinois 61801

A system of weakly coupled, geometrically nonlinear beams is examined. A Galerkin procedure is used to express the motions of the two beams in terms of their linearized flexural modes. Transient, impulsive excitations are considered, and the response of the system is analytically and numerically computed. For small values of a coupling nonlinear parameter, the vibrational energy injected into the system is proved to localize mainly at the directly forced beam, and only a small portion of this energy "leaks" to the unforced one. This passive, transient motion confinement is solely due to nonlinear localized modes of the unforced system, and it becomes more profound for stronger impulse excitations, and as the nonlinearity increases and/or the coupling stiffness connecting the two beams decreases. In the absence of nonlinearity, the injected vibrational energy is continuously transferred between the two beams, and thus no passive motion confinement is possible. Numerical integrations are used to verify the theoretical predictions. The implications of these findings on the passive and active isolation of flexible, nonlinear periodic structures are discussed.

I. Introduction

REPETITIVE structures are common in engineering practice. They consist of a number of identical substructures coupled by means of resilient elements. Such systems are commonly used in aerospace and turbomachinery applications: an assembly of helicopter blades can be regarded as a cyclic system of highly flexible (and hence geometrically nonlinear) coupled beams, periodically stiffened plates and shells are used for a long time as parts of aeroplane fuselages, and continuously shrouded bladed disk assemblies are essential parts of all turbomachines. In this work, a system consisting of two linearly coupled isotropic beams will be considered to model a two-helicopter blade assembly. Because of the flexibility of the beams, geometric and inertial nonlinearities occur, giving rise to a variety of nonlinear phenomena, having no counterpart in existing linear or linearized theories. In particular, for weak interblade coupling and/or strong blade nonlinearities, the assembly will be shown to possess nonlinear localized modes of vibration. The implementation of the mode localization properties of this system in the design for passive motion confinement of external disturbances is the main objective of this work.

In a number of recent works, the phenomenon of mode localization in "perturbed" linear periodic systems was investigated.[1–5] In these references it was shown that the (extended) normal modes of weakly coupled, symmetric linear systems become localized when weak perturbations of the periodicity are introduced. Linear mode localization was detected when the coupling between subsystems was of the order or smaller than the spread in natural frequencies of the component systems. The phenomenon of mode localization in discrete periodic oscillators with nonlinear stiffnesses was analytically and numerically studied in Refs. 6–8. This was accomplished using the notion of "nonlinear normal mode,"[9] i.e., of a free motion during which all coordinates of the system oscillate equiperiodically, reaching their extremum values at the same instant of time. As pointed out in other works,[10–12] although superposition of modal responses is not valid in nonlinear systems, forced nonlinear steady-state motions occur in the neighborhoods of the nonlinear normal modes (as in linear systems); thus, the examination of nonlinear normal modes provides valuable insight into the dynamic response of discrete nonlinear oscillators. Recently, the notion of "nonlinear normal mode" was extended to one-dimensional nonlinear continuous systems.[13,14]

In Ref. 8, a discrete cyclic system composed of n identical substructures possessing grounding nonlinearities of the third degree and linear coupling stiffnesses were studied. In all numerical examples, it was found that, for sufficiently weak coupling between substructures [of $\mathcal{O}(\varepsilon)$, $|\varepsilon|<<1$], the periodic system contained a "strongly" localized mode during only one coordinate vibrated with $\mathcal{O}(1)$ amplitude, the remaining coordinates oscillating with amplitudes of at least $\mathcal{O}(\varepsilon)$. Moreover, this "strongly localized" mode was found to be orbitally stable and thus physically realizable. Some additional results on nonlinear normal modes were recently reported in Ref. 15, where a new methodology for detecting nonlinear normal modes was described; this method is based on the computation of invariant manifolds for the motion and is valid even for systems with damping.

Localized modes in linear cyclic assemblies of beams modeling large space reflectors were investigated in Refs. 4, 5, and 16. Linear mode localization in such flexible structures occurred only in the presence of structural disorders, and the localized linear modes were investigated both analytically and numerically. It was shown that higher flexible modes were more susceptible to localization than lower ones. Moreover, the strength of the localization phenomenon was found to depend on the position of the coupling stiffness. A recent experiment[17] proved the existence of certain linear localized modes in a circular antenna with 12 flexible ribs and a gimbaled central hub. In accordance with existing theories, the "second bending group" of the antenna (ribs oscillating in their second flexible mode) was more effectively localized than the first group. Moreover, stronger localization was observed with increasing modal band. Mode localization in systems of flexible nonlinear beams was first examined in Ref. 18. In that work, a configuration of two coupled, geometrically nonlinear beams was investigated. A variety of localized modes was determined. The topology of the localized branches of modes was found to be greatly influenced by an "internal resonance" existing between the second and third linearized cantilever modes and by the position of the coupling stiffness.

A number of existing works investigate the spatial confinement of propagating disturbances in structures with localized modes. In Ref. 19, localization of propagating disturbances in one-dimensional disordered coupled oscillators and in beams with irregularly spaced constraints is studied using ensemble-averaging procedures. Analytic and numerical logarithmic averages for the transmission of disturbances along such systems were given. In Ref. 20, a wave propagation formulation for studying transmission in disor-

Received Jan. 30, 1993; accepted for publication March 4, 1994.

*Assistant Professor of Mechanical and Industrial Engineering and Bioengineering, Department of Mechanical and Industrial Engineering, 1206 W. Green Street. Member AIAA.

dered periodic systems is adopted. Multiplication of random transmission matrices is carried out to compute the "localization factors" inside the passbands of the unperturbed system. An extension of these statistical analyses was given in Ref. 21, where theoretical results on the localization factors were confirmed by Monte Carlo simulations. Localization of flexural propagating waves along a fluid-loaded plate with an irregular array of line attachments is presented in Ref. 22. A structural acoustics formulation is adopted in that work, and localization is studied by means of numerical simulations. Additional numerical computations of motion confinement of external disturbances due to mode localization were carried out for models of linear[4,5,23] and nonlinear[8] structures. These works demonstrated the beneficial effects of the mode localization phenomenon on the passive and/or active vibration isolation of periodic systems. This is because in a structure with localized modes the energy induced from an impulse in any of its substructures remains confined to that substructure and does not "spread" throughout the remaining system. Motion confinement due to nonlinear mode localization in impulsively loaded cyclic systems was demonstrated in Ref. 8, where the impulsive response of a nonlinear cyclic system with 50 degrees of freedom (DOF) was numerically computed using a finite element technique. For sufficiently weak coupling and no disorder, the energy of the impulse was confined to the point of its application, in contrast with the corresponding linear system where the energy "leaked" to the other components of the system. This motion confinement in the nonlinear system was attributed to the nonlinear localized modes, which did not exist in the corresponding linear structure.

The present work investigates the passive motion confinement properties of a system of two coupled, geometrically nonlinear beams. In Sec. II, the mathematical model is described and the nonlinear localized modes of the system are discussed. In Sec. III, both beams are forced to vibrate in their first cantilever mode, and motion confinement of a general class of induced impulses is proved analytically and numerically. An extension of the analysis for the case of three cantilever modes per beam is carried out in Sec. IV. A discussion of the implications of the main findings of this work is given in Sec. V.

II. Nonlinear Localized Modes of the Unforced System

The flexible system under consideration is shown in Fig. 1. The structure consists of two isotropic, linearly elastic beams of identical material properties and dimensions, which are coupled by means of a linear stiffness. Assuming no out-of-plane components of motion and increased beam flexibility, the nonlinear relation between curvature and transverse displacement and the longitudinal inertia of the beams give rise to geometric nonlinearities that can greatly influence the dynamic response.[24–27] Assuming that the beams are rigidly fixed to a non-moving rigid base and that weak coupling stiffness $K = \varepsilon k$ exists, where $|\varepsilon| \ll 1$, a rescaling of the transverse displacements, $v_p \to \varepsilon^{1/2} v_p$, leads to the following governing equations of motion:

$$v_{ptt} + v_{pxxxx} = -\varepsilon\Bigg[v_{px}(v_{px}v_{pxx})_x + (1/2)\,v_{px}\int_1^x\left(\int_0^s v_{px}^2\,\mathrm{d}u\right)_{tt}\mathrm{d}s\Bigg]_x$$

$$-\varepsilon\,(kL^4/EI)\,[v_p(l/L,t) - v_m(l/L,t)]\,\delta(x - l/L) + F_p(x,t)$$

$$u_p(x,t) = \mathcal{O}(\varepsilon), \qquad p, m = 1, 2, \qquad p \neq m \tag{1}$$

where v_p and u_p denote the transverse and longitudinal displacements of beam p, and x denotes the arclength per unit length of the two beams. In Eq. (1), t is the scaled time, defined by $t = \tau\,(EI/\rho L^4)^{1/2}$, where τ represents physical time, E the modulus of elasticity of the material of the beams, I the moment of inertia of the cross section of the beams about axes orthogonal to the plane of their motion, and ρ the material density per unit length. In Eqs. (1), no shear deformations of the cross section nor any rotary inertia effects are taken into account. The first nonlinear term in the right-hand side of Eqs. (1) is due to the nonlinear relation between the curvature and the transverse displacement, and the second nonlinear term represents the nonlinear coupling effects due to the nonlinear longitudinal inertia of the beam. Note that expressions (1) indicate that the longitudinal displacement $u(x, t)$ is of higher order than the transverse displacement $v(x, t)$ and therefore of much smaller magnitude and importance. In the following analysis, longitudinal motions are neglected.

For small values of ε, Eqs. (1) form a set of weakly nonlinear and weakly coupled partial differential equations. This set can be discretized by expressing the transverse displacements $v_p(x, t)$ in the following series form:

$$v_p(x,t) = \sum_{m=1}^{n} \phi_m(x)\,q_{pm}(t), \qquad p = 1, 2 \tag{2}$$

where the functions $\phi_m(x)$ are the normalized cantilever eigenfunctions of the linear parts of Eqs. (1) (corresponding to $\varepsilon = 0$) and $q_{pm}(t)$ new generalized coordinates. Substituting Eq. (2) into Eqs. (1), premultiplying by the ith normalized eigenfunction $\phi_i(x)$, integrating from $x=0$ to 1 with respect to the spatial variable, and using the orthogonality properties of the linearized eigenfunctions, one obtains the following set of ordinary differential equations for $q_{pi}(t)$:

$$\ddot{q}_{pi} + \omega_i^2 q_{pi} = -\varepsilon\Bigg\{\sum_{b=1}^{n}\sum_{k=1}^{n}\sum_{l=1}^{n}\Big[a_{iblk}q_{pb}q_{pk}q_{pl} + \frac{b_{ibkl}}{2}q_{pb}(q_{pk}q_{pl})_{tt}\Big] + \sum_{k=1}^{n}\gamma_{ki}\,[q_{pk} - q_{(p+1)k}]\Bigg\} + F_{pi}(t) \tag{3}$$

where the first subscript of q_{pi} represents the beam number, $p = 1$, 2, $p = 3 \equiv 1$, and the second subscript denotes the order of the linearized mode shape, $i = 1, 2, \ldots, n$. The various terms in Eq. (3) are defined as follows:

$$a_{ibkl} = \int_0^1 \phi_i\,[\phi_b'(\phi_k'\,\phi_l'')']'\,\mathrm{d}x$$

$$b_{ibkl} = \int_0^1 \phi_i\left(\phi_b'\int_1^x\int_0^\zeta \phi_b'\phi_b'\,\mathrm{d}\lambda\,\mathrm{d}\zeta\right)'\mathrm{d}x$$

$$\gamma_{ki} \equiv \frac{kL^4}{EI}\phi_k(l/L)\,\phi_i(l/L), \qquad F_{pi}(t) = \int_0^1 F_p(x,t)\,\phi_i\,\mathrm{d}x \tag{4}$$

where prime denotes differentiation with respect to the argument. The numerical values for some coefficients of Eqs. (4) are provided in Ref. 18.

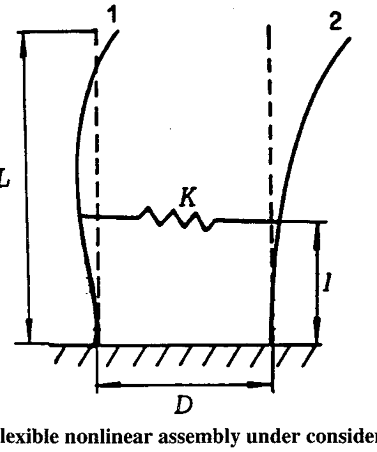

Fig. 1 Flexible nonlinear assembly under consideration.

The objective of the present work is to study the response of systems (1) and (3) due to general impulsive excitations $F_{pi}(t)$. Before analyzing the forced responses, it is of interest to review the nonlinear mode localization properties of the unforced system, corresponding to $F_{pi}(t)=0$ in Eq. (3). A detailed dynamic analysis of the unforced system was carried out in Ref. 18 by employing the method of multiple scales. To this end, the responses q_{pi} in Eq. (3) are expressed in the following form:

$$q_{pi}(t) = q_{pi}(T_0, T_1) = A_{pi}(T_1)\, e^{j\omega_i T_0} + \bar{A}_{pi}(T_1)\, e^{-j\omega_i T_0} + \mathcal{O}(\varepsilon) \tag{5}$$

where $T_0=t$ and $T_1=\varepsilon t$ are "fast" and "slow" time scales,[24] respectively, $A_{ip}(T_1)$ are complex amplitudes, $(\bar{\bullet})$ denotes the complex conjugate, and ω_i is the natural frequency of the ith linearized cantilever mode. The complex amplitudes in Eq. (5) are computed by substituting Eq. (5) into Eq. (4) and eliminating "secular terms" of the $\mathcal{O}(\varepsilon)$ equations, i.e., terms that lead to unbounded and, thus, nonuniformly valid solutions in time.[18] At this point, it is noted that a low-order "internal resonance" exists between the second and third flexural cantilever modes $\phi_2(x)$ and $\phi_3(x)$, since their corresponding linearized natural frequencies are nearly integrably related: $\omega_3 \sim 3\omega_2$. Such a low-order "internal resonance" is well known[24–27] to lead to nonlinear transfer of energy between the associated linearized modes and hence is expected to influence the nonlinear mode localization in the flexible system under consideration. To study the effects of this low-order internal resonance one introduces a "detuning" parameter σ defined as

$$\omega_3 = 3\omega_2 + \varepsilon\sigma \tag{6}$$

Parameter σ quantifies the closeness of the multiples of the natural frequencies of the modes participating in the internal resonance. Truncating expression (2) to three modes per blade ($n=3$), expressing the complex amplitudes as

$$A_{pi}(T_1) = (1/2)\, a_{pi}(T_1) \exp[j\theta_{pi}(T_1)]$$

where a_{pi} and θ_{pi} are real amplitudes and phases, substituting Eq. (5) into Eq. (3), and eliminating "secular terms," the following set of differential equations governing the amplitude and phase modulations is derived:

Mode 1:

$$\omega_1 a_{11}' = (1/2)\gamma_{11} a_{21} \sin(\theta_{21}-\theta_{11})$$

$$\omega_1 a_{21}' = -(1/2)\gamma_{11} a_{11} \sin(\theta_{21}-\theta_{11})$$

$$\omega_1 a_{11}\theta_{11}' = (1/2)\gamma_{11}[a_{11}-a_{21}\cos(\theta_{21}-\theta_{11})] - (a_{11}/8)\sum_{k=1}^{3}\eta_{1k}a_{1k}^2$$

$$\omega_1 a_{21}\theta_{21}' = (1/2)\gamma_{11}[a_{21}-a_{11}\cos(\theta_{11}-\theta_{21})] - (a_{21}/8)\sum_{k=1}^{3}\eta_{1k}a_{2k}^2 \tag{7a}$$

Mode 2:

$$\omega_2 a_{12}' = (1/2)\gamma_{22}a_{22}\sin(\theta_{22}-\theta_{12}) + (\xi/8)\, a_{13}a_{12}^2 \sin(\theta_{13}-3\theta_{12}+\sigma_1 T_1)$$

$$\omega_2 a_{22}' = (1/2)\gamma_{22}a_{12}\sin(\theta_{12}-\theta_{22}) + (\xi/8)\, a_{23}a_{22}^2 \sin(\theta_{23}-3\theta_{22}+\sigma_1 T_1)$$

$$\omega_2 a_{12}\theta_{12}' = (1/2)\gamma_{22}[a_{12}-a_{22}\cos(\theta_{22}-\theta_{12})] - (a_{12}/8)\sum_{k=1}^{3}\eta_{2k}a_{1k}^2 - (\xi/8)\, a_{13}a_{12}^2\cos(\theta_{13}-3\theta_{12}+\sigma_1 T_1)$$

$$\omega_2 a_{22}\theta_{22}' = (1/2)\gamma_{22}[a_{22}-a_{12}\cos(\theta_{12}-\theta_{22})] - (a_{22}/8)\sum_{k=1}^{3}\eta_{2k}a_{2k}^2 - (\xi/8)\, a_{23}a_{22}^2\cos(\theta_{23}-3\theta_{22}+\sigma_1 T_1) \tag{7b}$$

Mode 3:

$$\omega_3 a_{13}' = (1/2)\gamma_{33}a_{23}\sin(\theta_{23}-\theta_{13}) - (\delta/8)\, a_{12}^3 \sin(\theta_{13}-3\theta_{12}+\sigma_1 T_1)$$

$$\omega_3 a_{23}' = (1/2)\gamma_{33}a_{13}\sin(\theta_{13}-\theta_{23}) - (\delta/8)\, a_{22}^3 \sin(\theta_{23}-3\theta_{22}+\sigma_1 T_1)$$

$$\omega_3 a_{13}\theta_{13}' = (1/2)\gamma_{33}[a_{13}-a_{23}\cos(\theta_{23}-\theta_{13})] - (a_{13}/8)\sum_{k=1}^{3}\eta_{3k}a_{1k}^2 - (\delta/8)\, a_{12}^3\cos(\theta_{13}-3\theta_{12}+\sigma_1 T_1)$$

$$\omega_3 a_{23}\theta_{23}' = (1/2)\gamma_{33}[a_{23}-a_{13}\cos(\theta_{13}-\theta_{23})] - (a_{23}/8)\sum_{k=1}^{3}\eta_{3k}a_{2k}^2 - (\delta/8)\, a_{22}^3\cos(\theta_{23}-3\theta_{22}+\sigma_1 T_1) \tag{7c}$$

In Eqs. (7), primes denote differentiation with respect to the "slow time" T_1. The various parameters appearing in Eqs. (7) are defined as

$$\eta_{ii} \equiv 2\omega_i^2 b_{iiii} - 3a_{iiii}$$

$$\eta_{pi} \equiv 2b_{pipi}(\omega_p^2\omega_i^2) - 2(a_{ppii} + a_{piip} + a_{pipi})$$

$$\zeta \equiv b_{2232}(\omega_3-\omega_2)^2 + 2\omega_2^2 b_{2322} - a_{2223} - a_{2232} - a_{2322}$$

$$\delta \equiv 2\omega_2^2 b_{3222} - a_{3222} \tag{8}$$

The free nonlinear periodic solutions of the system are investigated by replacing the angle variables θ_{pi} with the new phase variables $\Phi_1 = \theta_{21}-\theta_{11}$, $\Phi_2 = \theta_{22}-\theta_{12}$, $\Phi_3 = \theta_{23}-\theta_{13}$, and $\Psi_1 = \theta_{13} - 3\theta_{12} + \sigma T_1$, and reducing Eqs. (7) to a set of 10 autonomous ordinary differential equations of first order.[18] The periodic solutions of the system are then obtained by imposing stationary conditions on the amplitude and phase variables, i.e., by setting $a_{pi}'=0$, $\Phi_i'=0$, and $\Psi_1'=0$ in the reduced set of equations, and solving the resulting set of stationary algebraic equations. This calculation was performed in Ref. 18, where it was found that certain of the periodic solutions of the system are localized. During such motions (localized normal oscillations), the modal amplitudes of one beam are much larger in magnitude than the corresponding amplitudes of the other beam, and thus the vibrational energy is spatially confined and nearly restricted to only one of the two subsystems. In a localized normal oscillation, the motions of the two beams are approximately given by

$$v_p(x,t) \approx \sum_{i=1}^{3}\{a_{pi}^*\cos[\omega_i t + \theta_{pi}^*(\varepsilon t)] + \mathcal{O}(\varepsilon)\}\,\phi_i(x) \qquad p = 1, 2 \tag{9}$$

where a_{pi}^* and $\theta_{pi}^*(\varepsilon t)$ denote the localized modal amplitudes and angles, obtained by solving the stationary equations. The stability of the periodic solutions (9) can be studied by Floquet analysis, i.e., by forming the appropriate system of linear variational equations in terms of the amplitude and phase modulations and computing the eigenvalues of the associated Floquet matrix.[24]

It turns out that there exist two basic classes of localized nonlinear modes in the system. The first category involves participation of only the first cantilever mode of the two blades, i.e., $a_{11}^* \neq 0$, $a_{21}^* \neq 0$, $a_{pi}^*=0$, $p=1, 2$, and $i=2, 3$, and the localized modes are

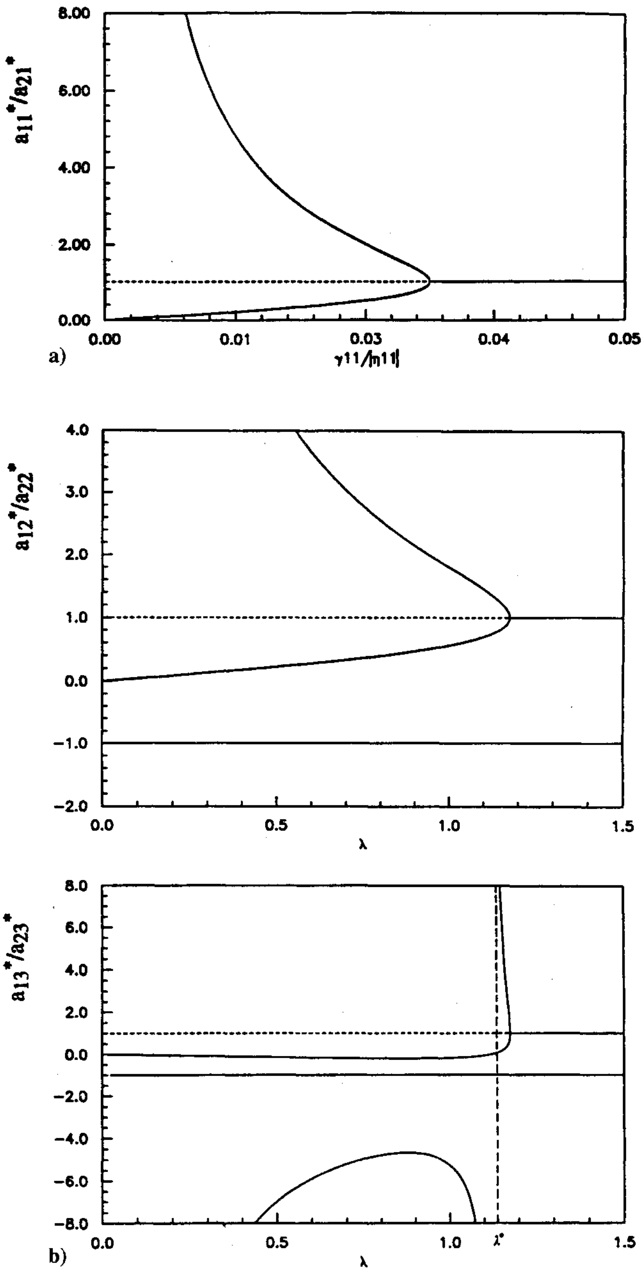

Fig. 2 Nonlinear mode localization for beams oscillating in a) their first cantilever mode and b) in their second and third cantilever modes; ———, stable modes and - - - - -, unstable modes.

depicted in Fig. 2a. Note that nonlinear localization depends on the ratio $r=\gamma_{11}/|\eta_{11}|$. From definitions (4) and (8) it can be seen that γ_{11} is a parameter related to the strength and position of the coupling stiffness, whereas η_{11} relates to the geometric nonlinearities of the beam. As $r\to 0$, the bifurcating modes become localized, $\lim_{r\to 0}\{a_{11}^*/a_{21}^*)\}=0$ or ∞, and the energy of the corresponding free motion is mainly confined to only one of the two beams (Fig. 2a). When r increases, the localized branches become nonlocalized and eventually coalesce with the antisymmetric mode in a Hamiltonian pitchfork bifurcation. This bifurcation point can be regarded as the point of generation of the nonlinear mode localization phenomenon. In physical terms, parameter r represents the ratio of coupling over nonlinear forces, and thus Fig. 2a shows that when both beams oscillate in their first bending mode, nonlinear mode localization occurs only when the coupling forces are weak and/or the beam nonlinearities are strong.

The second class of nonlinear localized modes involves participation of only the second and third cantilever modes, i.e., $a_{11}^* = a_{21}^*=0$, $a_{pi}^*\neq 0$, $p=1, 2$, and $i=2, 3$. In this case, the internal resonance between modes 2 and 3 greatly affects the topology of the localized branches. For $c=l/L=0.7650$ (where l is the coupling position), the branches of localized modes are depicted in Fig. 2b. In each of the two diagrams the ratio of the modal amplitudes (a_{1i}^*/a_{2i}^*), $i=2, 3$ is plotted vs the parameter $\lambda=(kL^4/EI)/a_{3223}$. Again, it is observed that $\lim_{\lambda\to 0}\{a_{1i}^*/a_{2i}^*\}=0$ or ∞, $i=2, 3$, i.e., that as the coupling decreases and/or the nonlinearity increases nonlinear mode localization occurs. As λ increases, the localized modes become nonlocalized, until they coalesce with the symmetric mode in a pitchfork bifurcation. An interesting feature of mode localization in the presence of internal resonance is its essential dependence on the position of the coupling stiffness. Indeed, when $c=l/L$ is close to 0.783, the value corresponding to the node of the second (lower) cantilever mode, a complicated sequence of bifurcations of certain solution branches takes place.[18] Additionally, it can be shown that high modes are more susceptible to nonlinear mode localization than lower ones. In Fig. 3, the values of the coupling stiffness at the points of generation of the localized mode branches are plotted as functions of the position of the coupling stiffness. Both categories of localized solutions are depicted, and it can be seen that localization for modes 2 and 3 is generated at much higher values of the coupling stiffness than foı mode 1. Similar results hold for higher modes. It is concluded that if the coupling stiffness is low enough to localize the first cantilever mode, then it is sufficient to localize all higher modes; this result is in full agreement with existing theories on mode localization of disordered, linear beam assemblies.[4,5,16,17,23]

The results presented in this section establish the existence of stable nonlinear localized modes in the unforced flexible assembly of Fig. 1. These modes were found to exist only for sufficiently small coupling stiifnesses and/or large nonlinear forces. Moreover, the nonlinear localization phenomenon becomes much more profound for high-mode vibrations. In the next sections it will be shown that, due to nonlinear mode localization, a spatial confinement of a general class of externally induced transient impulses results. Thus, it will be proven that the symmetric two-beam nonlin-

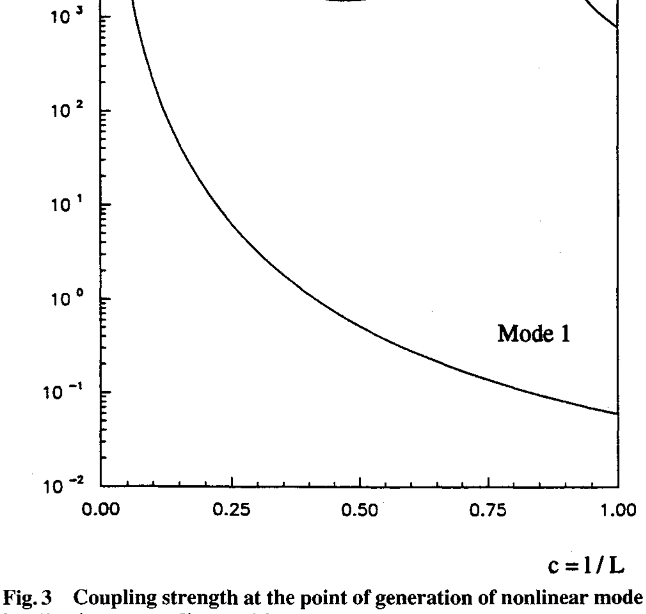

Fig. 3 Coupling strength at the point of generation of nonlinear mode localization vs coupling position.

ear system possesses passive motion confinement characteristics, a result with no counterpart in existing linear theories.

III. Impulsive Motion Confinement, Single-Mode Vibrations

Passive confinement of externally induced impulses in a discrete nonlinear cyclic system was studied in Ref. 8, by employing purely numerical techniques. To initiate the study of the motion confinement properties of the nonlinear flexible system of Fig. 1, excitations of the following form are assumed to be applied to the two beams:

$$F_1(x,t)=(1/\varepsilon)f_1(t)=\phi_1(x) \text{ for } 0\le t<\varepsilon D$$

$$F_1(x,t)=0 \text{ for } t\ge\varepsilon D,\qquad F_2(x,t)=0,\qquad 0\le t<\infty \tag{10}$$

Thus, a general impulsive excitation of duration εD is assumed to act on beam 1, with a spatial distribution identical to that of the first linearized cantilever mode. Beam 2 is not excited at this stage. Forcing functions with more general spatial distributions will be considered in the next section. Expressing the displacements $v_p(x,t)$, $p=1,2$, in terms of the linearized cantilever modes, one obtains the discretized set of forced ordinary differential equations (3). Taking into account definitions (4) and (10), the forcing terms in equations (3) assume the form

$$(1/\varepsilon)F_{pi}(t)=(1/\varepsilon)\int_0^1 f_1(t)\phi_i^2(x)\,\mathrm{d}x\,\delta_{p1}\delta_{i1}\quad\text{for } 0\le t<\varepsilon D$$

$$F_{pi}(t)=0\quad\text{for}\quad t\ge\varepsilon D \tag{11}$$

where δ_{ij} is Kroenecker's symbol. It is therefore concluded that, by using the impulse distributions (10), it is ensured that only the first cantilever mode of beam 1 is directly excited by the forcing distributions (10). It is of interest to study the transfer of the energy of the impulse from the directly excited mode to the other modes of the system; clearly, spatial motion confinement of the external impulse is achieved if and only if minimal amounts of vibrational energy eventually "leak" to the modes of the unforced beam 2.

In the previous section, it was found that a low-order internal resonance exists between the second and third cantilever modes; moreover, the first cantilever mode was found not to possess any nonlinear coupling with any higher modes. Hence, no energy transfer is expected to occur from the directly excited first mode of beam 1 to any other higher modes of the two beams, and thus the only possible energy exchange is anticipated to take place only between the first cantilever modes of the two beams. This theoretical prediction will be verified in the following analysis. The dynamics of the forced system (3) will now be analyzed by examining the modal responses in two distinct phases. For the sake of simplicity, the analysis is limited to $n=3$ cantilever modes per beam.

Phase 1, $0\le t<\varepsilon D$

During this phase, the applied force is nonzero, and the response is asymptotically approximated by introducing the new time T, defined by $t=\varepsilon T$. The range of values of the new time variable during this phase of the motion is $0\le T<D$. Expressing the time derivatives in Eq. (3) in terms of the new variable T, the governing equations for the modal amplitudes are written as follows:

Mode 1:

$$\frac{\mathrm{d}^2q_{p1}}{\mathrm{d}T^2}=\varepsilon\left[-\sum_{b=1}^{3}\sum_{k=1}^{3}\sum_{l=1}^{3}\frac{b_{1bkl}}{2}q_{pb}(q_{pk}q_{pl})_{TT}+\hat{p}_1(T)\delta_{p1}\right]$$
$$-\varepsilon^2\omega_1^2q_{p1}-\varepsilon^3\left\{\sum_{b=1}^{3}\sum_{k=1}^{3}\sum_{l=1}^{3}a_{1blk}q_{pb}q_{pk}q_{pl}\right.$$
$$\left.+\sum_{k=1}^{3}\gamma_{ik}[q_{pk}-q_{(p+1)k}]\right\},\qquad p=1,2 \tag{12}$$

with similar expressions holding for the modal displacements q_{p2} and q_{p3}, $p=1,2$, of the higher modes. Complementing Eqs. (12) is the set of initial conditions $q_{pi}(0)=0$, $\mathrm{d}[q_{pi}(0)]/\mathrm{d}T=0$, $p=1,2$, $i=1,2,3$, since at $t=T=0$ the system is assumed to be at rest. In Eqs. (12), all depended variables are functions of T, and the new forcing function is defined as

$$\hat{p}_1(T)\equiv F_{11}(\varepsilon T) \tag{13}$$

The response of system (12) is approximated using regular perturbation expansions, i.e., by expressing the responses in the form

$$q_{pi}(T)=\sum_{m=1}^{\infty}\varepsilon^m q_{pi}^{(m)}(T)$$

and substituting in Eqs. (12). By matching the coefficients of respective powers of ε, one determines the various orders of approximation. Omitting the calculations, and transforming in terms of the original time variable, the response of the system during this phase is computed as

$$q_{11}(t)=\varepsilon\int_0^{(t/\varepsilon)}\int_0^{\eta}\hat{p}_1(s)\,\mathrm{d}s\,\mathrm{d}\eta+\mathcal{O}(\varepsilon^3)$$

$$\dot{q}_{11}(t)=\int_0^{(t/\varepsilon)}\hat{p}_1(s)\,\mathrm{d}s+\mathcal{O}(\varepsilon^2) \tag{14}$$

$$q_{ij}(t)=\mathcal{O}(\varepsilon^4),\qquad \dot{q}_{ij}(t)=\mathcal{O}(\varepsilon^3),\qquad\text{otherwise}$$

Hence, the analysis predicts that for $0\le t<\varepsilon D$ (the duration of the impulse) the response of the system is mainly determined by the impulse itself and not by any structural parameters (the system "does not have time to oscillate"). Note that the velocity of the directly excited mode is of $\mathcal{O}(1)$, whereas the response of all unforced modes are orders of magnitudes smaller than that of the directly forced mode. The resulting physical motions of the two beams are given by

$$v_1(x,t)\approx\varepsilon^{1/2}\phi_1(x)q_{11}(t)+\mathcal{O}(\varepsilon^{7/2}),\qquad v_2(x,t)\approx\mathcal{O}(\varepsilon^{9/2})$$
$$\text{for}\quad 0\le t<\varepsilon D \tag{15}$$

where the previously introduced scaling of the transverse displacements $v_p(x,t)\to\varepsilon^{1/2}v_p(x,t)$, $p=1,2$, was taken into account.

Phase 2, $t\ge\varepsilon D$

During this phase of the motion, the impulse ceases to apply, and thus the system performs free oscillations, with initial conditions determined from Eqs. (14). Introducing the time translation $\hat{t}=t-\varepsilon D$, the governing equations (3) are expressed as

$$\ddot{q}_{pi}+\omega_i^2q_{pi}=-\varepsilon\left\{\sum_{b=1}^{3}\sum_{k=1}^{3}\sum_{l=1}^{3}\left[a_{iblk}q_{pb}q_{pk}q_{pl}\right.\right.$$
$$\left.\left.+\frac{b_{ibkl}}{2}q_{pb}\frac{\mathrm{d}^2(q_{pk}q_{pl})}{\mathrm{d}\hat{t}^2}\right]+\sum_{k=1}^{3}\gamma_{ik}[q_{pk}-q_{(p+1)k}]\right\}$$
$$p=1,2,\qquad i=1,2,3 \tag{16}$$

where differentiation is carried out with respect to $\hat{t}$, and $q_{pi}=q_{pi}(\hat{t})$. From Eqs. (14), the set of initial conditions complementing Eqs. (16) is

$$q_{11}(0)=\varepsilon\int_0^{D}\int_0^{\eta}\hat{p}_1(s)\,\mathrm{d}s\,\mathrm{d}\eta+\mathcal{O}(\varepsilon^3)$$

$$\dot{q}_{11}(0)=\int_0^{D}\hat{p}_1(s)\,\mathrm{d}s+\mathcal{O}(\varepsilon^2)$$

and $q_{pi}(0)=\mathcal{O}(\varepsilon^4)$, and $\dot{q}_{pi}(0)=\mathcal{O}(\varepsilon^3)$, otherwise. Since Eqs. (16) represent free oscillations of the system, their solutions can be analytically approximated by the multiple scales singular perturbation analysis outlined in Sec. II. To this end, the modal responses are expressed according to Eq. (5), with time scales $T_0=\hat{t}$ and $T_1=\varepsilon\hat{t}$. Introducing the transformations $A_{pi}(T_1)=(1/2)\,a_{pi}(T_1)\,e^{j\theta_{pi}(T_1)}$, $p=1,2$, $i=1,2,3$, the modulation equations (7) governing the real amplitudes $a_{pi}(T_1)$ and angles $\theta_{pi}(T_1)$ are obtained. To compute the amplitude and phase modulations of the response, one should solve Eqs. (7), with initial conditions

$$a_{11}(0) = -(1/\omega_1)\int_0^D \hat{p}_1(s)\,\mathrm{d}s$$

$a_{21}(0)=0$, $\theta_{11}(0)=\pm\pi/2$, $\theta_{21}(0)=0$, $a_{pi}(0)=0$, otherwise. The resulting physical motions of the beams are then approximated by

$$v_p(x,t)\approx\varepsilon^{1/2}\sum_{i=1}^{3}\left(a_{pi}[\varepsilon(t-\varepsilon D)]\cos\{\omega_i(t-\varepsilon D)+\theta_{pi}[\varepsilon(t-\varepsilon D)]\}+\mathcal{O}(\varepsilon)\right)\phi_i(x)\,,\qquad t\ge\varepsilon D,\quad p=1,2 \tag{17}$$

Considering the structure of Eqs. (7b) and (7c), it can be mathematically proven that if $a_{12}(0)=a_{13}(0)=a_{22}(0)=a_{23}(0)=0$, then $a_{12}(T_1)=a_{13}(T_1)=a_{22}(T_1)=a_{23}(T_1)=0$, $\forall T_1$. Therefore, in this case, the modulation equations (7) can be reduced into the following set:

$$a'_{11}=(\gamma/2\omega)\,a_{21}\sin(\theta_{21}-\theta_{11})$$

$$a'_{21}=-(\gamma/2\omega)\,a_{11}\sin(\theta_{21}-\theta_{11})$$

$$a_{11}\theta'_{11}=[(3\alpha/8\omega_1)-(\beta\omega_1/4)]\,a_{11}^3+(\gamma/2\omega)\,a_{11}-(\gamma/2\omega)\,a_{21}\cos(\theta_{21}-\theta_{11})$$

$$a_{21}\theta'_{21}=[(3\alpha/8\omega_1)-(\beta\omega_1/4)]\,a_{21}^3+(\gamma/2\omega)\,a_{21}-(\gamma/2\omega)\,a_{11}\cos(\theta_{21}-\theta_{11}) \tag{18a}$$

where primes denote differentiation with respect to the "slow time" T_1, and the simplified notation, $\alpha\equiv a_{1111}$, $\beta\equiv b_{1111}$, and $\gamma\equiv\gamma_{11}$, is adopted from now on. Hence, it is proven that the only possible energy transfer is between the first modes of the two beams and that no other energy exchange involving higher modes occurs. To investigate the energy transfer between the modes of beams 1 and 2, one needs to integrate Eqs. (18a). Define at this point the quantity

$$J=\gamma/\{[(3\alpha/2)-(\beta\omega_1^2)]\,\rho\}$$

where

$$\rho=(2\omega_1)^{-1}\int_0^D\hat{p}_1(s)\,\mathrm{d}s$$

Parameter J is recognized as the ratio of the coupling over the product of nonlinear forces and the energy of input ρ. It will be now shown that, for $J<<1$, the response of the system can be analytically approximated. This is achieved by expressing the amplitudes and angles as

$$a_{p1}(T_1)=\sum_{m=0}^{\infty}J^m a_{p1}^{(m)}(T_1)$$

$$\theta_{p1}(T_1)=\sum_{m=0}^{\infty}J^m\theta_{p1}^{(m)}(T_1)\qquad p=1,2$$

and substituting into Eq. (18a). Matching terms proportional to the same power of J leads to the following analytical expressions for the amplitude modulations:

$$a_{11}(T_1)=\pm\left(2\rho-(J^2/\rho)\sin^2\{[(3\alpha/4\omega_1)-(\beta\omega_1/2)]\,\rho^2T_1\}+\mathcal{O}(J^3)\right)$$

$$a_{21}(T_1)=\pm\left(-2J\sin\{[(3\alpha/4\omega_1)-(\beta\omega_1/2)]\,\rho^2T_1\}+\mathcal{O}(J^2)\right)\qquad(J<<1) \tag{18b}$$

Similar analytical expressions hold for the angles $\theta_{p1}(T_1)$. Solutions (18b) predict that when $J<<1$, the transient impulsive response of the system is mainly confined to the directly excited blade, since $a_{11}(T_1)>>a_{21}(T_1)$. Now, based on the results of Sec. II, the condition $J<<1$ (weak coupling and/or strong nonlinearities and/or strong impulsive excitations) is also recognized as the condition for the existence of localized nonlinear modes in the system. It is therefore concluded that when the system possesses nonlinear localized modes, it also possesses passive motion confinement properties: when an external impulse acts at one beam of the system, the disturbance remains spatially confined to its point of application, and only a small portion of the injected energy leaks to the unforced beam. Moreover, from Eq. (18b), it is predicted that the responses of the forced and unforced beams contain $\mathcal{O}(J^2)$ and $\mathcal{O}(J)$ amplitude modulations, respectively. This is consistent with energy conservation considerations. Indeed, from Eq. (18b), a direct computation gives $a_{11}^2(T_1)+a_{21}^2(T_1)=4\rho^2+\mathcal{O}(J^3)$. Correct to $\mathcal{O}(\varepsilon)$, this relation can be shown to represent conservation of energy of the free, undamped system under consideration.[28] It must be stated that the analytic approximations (18b) hold only for small values of the quantity J.

As J increases to finite values, i.e., when the coupling increases and/or the nonlinear forces decrease, one needs to resort to numerical integrations to compute the solutions of system (18a). The numerical integrations verify the theoretical predictions. The numerically computed amplitude modulations for $\alpha=40.44$, $\beta=4.59$, $\varepsilon=0.5$, $\omega_1^2=12.38$ (rad/s)^2, and $\rho=0.1421$ are depicted in Fig. 4. For the sake of clarity, only the "lower" pair of modulations is shown. The parameter J was varied by changing the coupling variable γ. For $J<<1$, the modal amplitude of the unforced beam 2 is small, whereas the directly excited beam undergoes a modulated oscillation close to its initial amplitude value,

$$a_{11}(0)=-(1/\omega_1)\int_0^D\hat{p}_1(s)\,\mathrm{d}s\,(-2\rho)$$

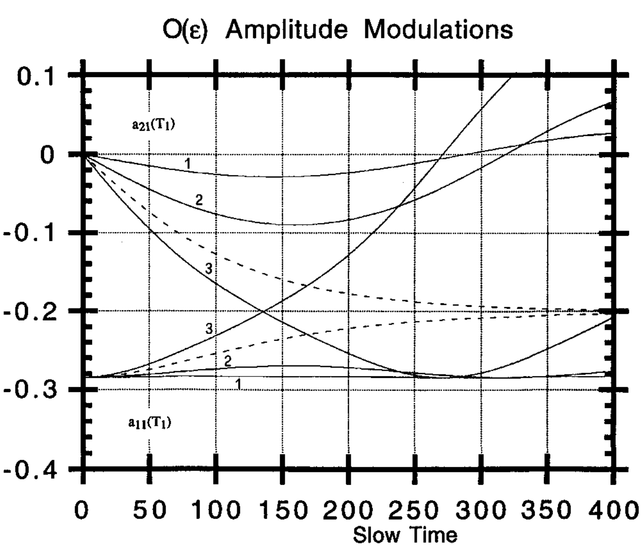

Fig. 4 Single-mode oscillations and amplitude modulations computed by numerically integrating the reduced set of modulation equations (18a): 1) $J=0.0142$, 2) $J=0.0426$, 3) $J=0.0924$, and -----, $J=J_{cr}=0.0711$.

Hence, for $J<<1$, passive motion confinement of the impulse to the directly excited beam is observed. As J increases, the amplitude a_{21} of the unforced beam grows, indicating an increased transfer of energy out of the directly excited beam or, equivalently, a diminishing of the motion confinement capacity of the system. At a critical value, $J=J_{cr}=\rho/2$, all vibrational energy of the directly excited beam is eventually transferred to the unforced one. For values of J above the critical value, energy is continuously transferred between the two beams, and the system does not possess passive motion confinement properties anymore. To verify the results of the multiple scales analysis, an impulsive distributed excitation of magnitude

$$F_1(x,t) = 5\phi_1(x) \Rightarrow (1/\varepsilon)F_{11}(t) = \int_0^1 10\phi_i\,dx$$

and duration $\varepsilon D=0.1$ s was applied to beam 1, and the structural parameters were assigned the values $\varepsilon=0.5$, $a_{1111}=40.44$, $b_{1111}=4.59$, $\gamma_{11}=0.02$, $\omega_1=3.51$ (rad/s), and $J=0.0367<<1$; the response was numerically computed by directly integrating the differential equations of motion (3) with $q_{12}=q_{13}=q_{22}=q_{23}=0$, and assuming zero initial conditions at $t=0$. In Fig. 5a the responses of the two beams are shown as functions of time, and in Fig. 5b a projection of the phase space of the motion is depicted. Note that the energy of the injected impulse is mainly confined to the directly forced beam, according to theoretical predictions. The amplitude of the unforced beam can be further diminished by decreasing the coupling stiffness and/or increasing the nonlinear coefficients. For comparison purposes, the theoretically predicted amplitude modulations (18b) are also presented in Fig. 5c. Clearly, the asymptotic theory agrees well with the numerical computations for this low value of J. Note that, in the absence of nonlinearities, all injected energy is continuously transferred between the forced and unforced beams, in the well-known "beat phenomenon." Hence, the detected passive motion confinement phenomenon is attributed to a balance between linear coupling, geometric nonlinearities of the system, and impulse strength.

Summarizing, the results of this section prove that, for small values of the parameter J (i.e., for small coupling stiffness and/or large nonlinear forces), impulsive forces with spatial distributions identical to the first cantilever mode become spatially confined to the directly excited beam. The only possible energy exchange in this case is between the first modes of the two beams, and no higher modes are indirectly excited. As J increases, the amount of energy leaking to the unforced beam also increases, and the passive motion confinement of the induced disturbance becomes less profound. For J greater than a critical value no motion confinement becomes possible anymore. In the next section, the effects of higher cantilever modes on the motion confinement properties of the system are investigated.

IV. Impulsive Motion Confinement, Multimode Vibrations

To study the motion confinement properties of the system for applied impulses of general spatial distribution, the forcing terms in the equations of motion (1) are now assumed in the form

$$F_1(x,t)=(1/\varepsilon)f_1(x,t) \quad \text{for } 0\le t<\varepsilon D$$
$$F_1(x,t)=0 \quad \text{for } t\ge\varepsilon D$$
$$F_2(x,t)=0, \quad 0\le t<\infty \tag{19}$$

leading to the following modal excitations for the discretized equations (3):

$$(1/\varepsilon)F_{1i}(t) = (1/\varepsilon)\int_0^1 f_1(x,t)\phi_i(x)\,dx \quad \text{for } 0\le t<\varepsilon D$$
$$F_{1i}(t) = 0 \quad \text{for } t\ge\varepsilon D$$
$$F_{2i}(t)=0, \quad i=1,2,3 \tag{20}$$

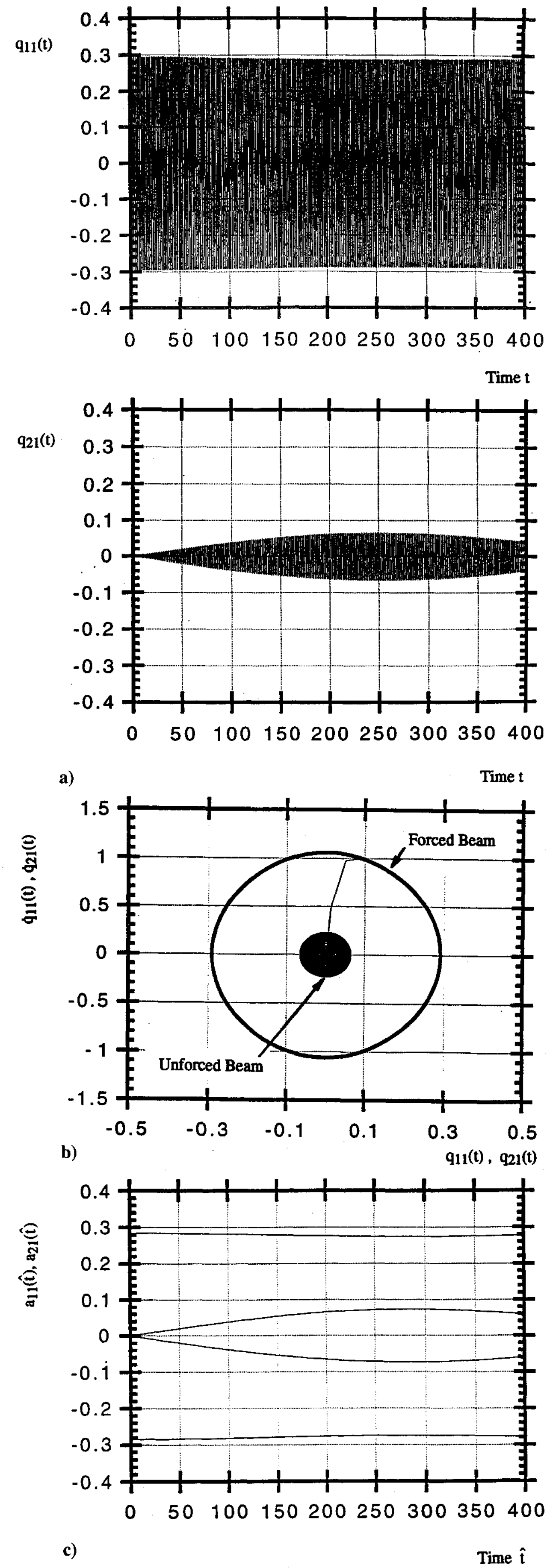

Fig. 5 Single-mode oscillations and amplitude modulations computed by a) direct integrations of the equations of motion and time responses, b) direct integrations of the equations of motion and responses in a projection of the phase space, and c) theoretical results, Eq. (18b).

The modal responses can be computed by solving the set of Eqs. (3), with zero initial conditions at $t=0$. To achieve this, the analytical methodology employed in the previous section is used, and the dynamic response is computed in two distinct stages.

Phase 1, $0 \le t < \varepsilon D$

During this phase, the applied force is nonzero, and the regular perturbation analysis outlined in the previous section is followed to show that

$$q_{1i}(t) = \varepsilon\int_0^{(t/\varepsilon)}\int_0^{\eta}\hat{p}_1(s)\ ds\ d\eta + \mathcal{O}(\varepsilon^3)$$

$$\dot{q}_{1i}(t) = \int_0^{(t/\varepsilon)}\hat{p}_1(s)\ ds + \mathcal{O}(\varepsilon^2)$$

$$q_{2i}(t) = \mathcal{O}(\varepsilon^4), \qquad \dot{q}_{2i}(t) = \mathcal{O}(\varepsilon^3), \qquad i=1,2,3 \tag{21a}$$

$$\hat{p}_i(T) \equiv F_{1i}(\varepsilon T) \tag{21b}$$

Expressions (21) and (22) are used to determine the initial conditions for the ensuing free response of the system during the next stage of the motion. The physical motions of the beams during this stage of the motion are given by

$$v_1(x,t) \approx \phi_1(x)q_{11}(t) + \phi_2(x)q_{12}(t) + \phi_3(x)q_{13}(t) + \mathcal{O}(\varepsilon^3)$$

$$v_2(x,t) \approx \mathcal{O}(\varepsilon^4), \qquad \text{for } 0 \le t < \varepsilon D \tag{22}$$

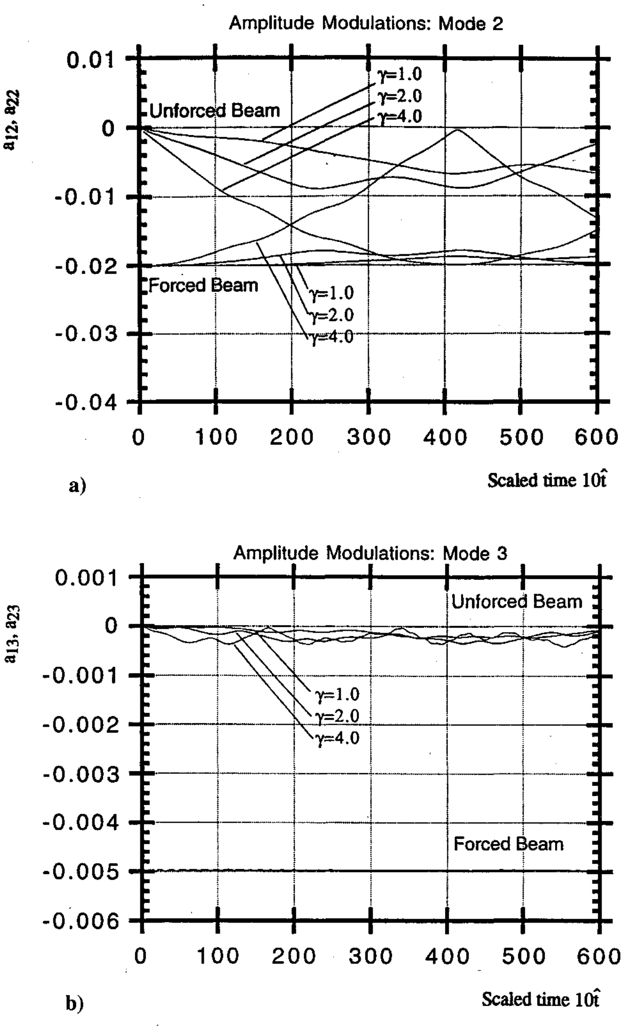

Fig. 6 Multimode oscillations and amplitude modulations computed by numerically integrating the general modulation equations (7).

Phase 2, $t \ge \varepsilon D$.

During this phase of the motion, the impulse ceases to apply, and the system performs free oscillations. Introducing again the time translation $\hat{t} = t - \varepsilon D$, expressing the modal amplitudes according to Eq. (5), setting

$$A_{pi}(T_1) = (1/2)\ a_{pi}(T_1)\exp[j\theta_{pi}(T_1)],\ p=1,2,\ i=1,2,3$$

with $T_1 = \varepsilon\hat{t}$, and eliminating the "secular terms" in the $\mathcal{O}(\varepsilon)$ equations of motion, one obtains the governing modulation equations (7). In this case, the initial conditions for the modulation equations are given by

$$a_{1i}(0) = -(1/\omega_i)\int_0^D \hat{p}_i(s)\ ds$$

$$a_{2i}(0) = 0, \qquad \theta_{1i}(0) = \pm\pi/2$$

$$\theta_{2i}(0) = 0, \qquad i=1,2,3$$

The physical responses of the two beams are given by expressions (17). Assuming that the coupling stiffness is positioned at $l=L$ (see Fig. 1), one obtains that $\gamma_{11}=\gamma_{22}=\gamma_{33}=\gamma$. The numerical values of the coefficients η_{ij} of Eqs. (7) are listed in the Appendix, and numerical solutions of these equations for $\varepsilon=0.5$, $a_{11}(0)=-0.2842$, $a_{12}(0)=-0.0200$, and $a_{13}(0)=-0.0050$ are depicted in Fig. 6 for varying values of the coupling parameter γ. The solutions of the modulation equations occur in opposite positive-negative pairs, and in Fig. 6 only the negative values of the modulations are presented.

In Fig. 6a, the amplitude modulations of the second modes of the forced and unforced beams are presented. Note that motion confinement of the second mode exists even at relatively high values of the coupling parameter ($\gamma=1.0, 2.0$), whereas complete energy transfer between the second modes of the two beams occurs for $\gamma=4.0$. In Fig. 6b, the corresponding amplitude modulations for mode 3 are shown, and it is observed that very strong spatial confinement of the energy of mode 3 occurs even for values of the coupling parameter as high as $\gamma=4.0$. Similar calculations (not shown here) indicate that complete transfer of energy between the first modes of the two beams occurs only at values of the coupling as high as $\gamma=4.0$, whereas for $\gamma=2.0$, some small spatial confinement of the energy of mode 1 of the forced beam still exists. These values of γ should be compared with the critical value $\gamma=0.03873$ (see previous section), for which complete energy transfer occurs between the first modes of the beams, when they alone are excited.

It is concluded that when three modes of the directly forced beam are simultaneously excited, spatial localization of the impulse occurs over a wider range of values of the coupling parameter, and thus the system possesses more profound motion confinement characteristics. Moreover, higher modes provide more effective passive confinement of the induced motion, a feature that is to be expected, since such modes localize much easier than lower ones.

V. Discussion

In this work it was proved that a geometrically nonlinear and weakly coupled system of beams can possess passive spatial motion confinement properties. The presented analysis employed regular and singular perturbation techniques, combined with numerical integrations of the corresponding modulation equations. For motions of the beams in their first cantilever mode, it was found that spatial motion confinement of the induced disturbance occurs when the linear coupling is sufficiently small and/or the nonlinear effects large and/or the impulse excitation is strong. In fact, the weaker the impulse strength, the stronger the ratio of coupling to nonlinear forces should be to achieve passive motion confinement. When higher modes are taken into account, the motion confinement becomes more evident.

Although the analysis presented herein dealt with a configuration of only two beams, the obtained results can be extended to a more general class of multiple connected flexible systems with or without symmetry. By designing such systems so that their coupling stiffnesses are small or/and their geometric nonlinearities large, applied impulses are ensured not to "spread" through the entire structure but to remain confined to the subsystem where they are originally applied. Note that this confinement of vibrational energy is purely passive and is solely due to orbitally stable localized nonlinear modes of the system. The implications of such a dynamical feature are profound. Indeed, a system whose inherent dynamics lead to motion confinement of external disturbances is much more amenable to active or passive isolation than a structure possessing "extended" dynamic modal responses (i.e., motions during which all of its substructures vibrate with finite amplitudes). Therefore, the class of nonlinear systems under consideration in this work are expected to possess enhanced controllability features, since in the planning of passive or active control algorithms one needs only consider the dynamic response of only a limited number of substructures instead of the whole system; however, issues of performance, "spill-over," and robustness must be addressed in such active designs. The development of active control techniques for shock and vibration isolation of the class of nonlinear systems discussed in this work is the focus of current research by the author and co-workers.

Appendix: Numerical Values of the Coefficients of Eqs. (7)

Using the definitions (8) and (4), and taking into account that the linearized cantilever eigenfunctions are given by

$$\phi_i(x) = \cosh \psi_i x - \cos \psi_i x + N(\psi_i)(\sinh \psi_i x - \sin \psi_i x) \quad \text{(A1)}$$

where $N(\psi_i) = (\sin \psi_i - \sinh \psi_i)/(\cos \psi_i + \cosh \psi_i)$, and $\cos \psi_i \cosh \psi_i = -1$, the various coefficients in Eqs. (7) assume the following numerical values:

$$\eta_{11} = -7.69, \quad \eta_{12} = \eta_{21} = 1114.79, \quad \eta_{13} = \eta_{31} = 15916.42$$

$$\eta_{22} = 100271.71, \quad \eta_{23} = \eta_{32} = 75688.97, \quad \eta_{33} = 6816895.85$$

$$\xi = -13715.76, \quad \delta = -7566.34 \quad \text{(A2)}$$

Acknowledgments

This work was supported by National Science Foundation Grant MSS 92-07318. Devendra Garg was the grant monitor. The author would like to thank Melvin King (his graduate research assistant) for his help with Fig. 3 and the numerical results listed in the Appendix.

References

[1]Hodges, C. H., "Confinement of Vibration by Structural Irregularity," *Journal of Sound and Vibration*, Vol. 82, No. 3, 1982, pp. 411–424.

[2]Pierre, C., and Dowell, E. H., "Localization of Vibrations by Structural Irregularity," *Journal of Sound and Vibration*, Vol. 114, No. 3, 1987, pp. 549–564.

[3]Wei, S.-T., and Pierre, C., "Localization Phenomena in Mistuned Assemblies with Cyclic Symmetry Part I: Free Vibrations & II: Forced Vibrations," *ASME Journal of Vibration, Acoustics and Reliability in Design*, Vol. 110, 1988, pp. 429–448.

[4]Bendiksen, O. O., "Mode Localization Phenomena in Large Space Structures," *AIAA Journal*, Vol. 25, No. 9, 1987, pp. 1241–1248.

[5]Cornwell, P. J., and Bendiksen, O. O., "Localization of Vibrations in Large Space Reflectors," *AIAA Journal*, Vol. 27, No. 2, 1989, pp. 219–226.

[6]Vakakis, A. F., "Nonsimilar Normal Oscillations in a Strongly Nonlinear Discrete System," *Journal of Sound and Vibration*, Vol. 158, No. 2, 1992, pp. 341–361.

[7]Vakakis, A. F., and Cetinkaya, C., "Mode Localization in a Class of Multi-Degree-of-Freedom Nonlinear Systems with Cyclic Symmetry," *SIAM Journal on Applied Mathematics*, Vol. 53, 1993, pp. 265–282.

[8]Vakakis, A. F., Nayfeh, T., and King, M. E., "A Multiple-Scales Analysis of Nonlinear, Localized Modes in a Cyclic Periodic System," *ASME Journal of Applied Mechanics*, Vol. 60, No. 2, 1993, pp. 388–397.

[9]Rosenberg, R. M., "On Nonlinear Vibrations of Systems with Many Degrees of Freedom," *Advances in Applied Mechanics*, Vol. 9, 1966, pp. 155–242.

[10]Caughey, T. K., and Vakakis, A. F., "A Method for Examining Steady State Solutions of Forced Discrete Systems with Strong Non-Linearities," *International Journal of Non-Linear Mechanics*, Vol. 26, 1991, pp. 89–103.

[11]Vakakis, A. F., and Caughey, T. K., "A Theorem on the Exact Nonsimilar Steady-States of a Nonsimilar Oscillator," *ASME Journal of Applied Mechanics*, Vol. 59, 1992, pp. 418–424.

[12]Vakakis, A. F., "Fundamental and Subharmonic Resonances in a System with a '1-1' Internal Resonance," *Nonlinear Dynamics*, Vol. 3, 1992, pp. 123–143.

[13]Shaw, S. W., and Pierre, C., "Normal Modes of Vibration for Nonlinear Continuous Systems," *Journal of Sound and Vibration* (to be published).

[14]King, M. E., and Vakakis, A. F., "An Energy-Based Formulation for Computing Nonlinear Normal Modes in Undamped Continuous Systems," *ASME Journal of Vibration and Acoustics* (to be published).

[15]Pierre, C., and Shaw, S., "Mode Localization due to Symmetry-Breaking Nonlinearities," *International Journal of Bifurcation and Chaos*, Vol. 1, No. 2, 1991, pp. 471–475.

[16]Pierre, C., and Cha, P., "Strong Mode Localization in Nearly Periodic Disordered Structures," *AIAA Journal*, Vol. 27, No. 2, 1989, pp. 227–241.

[17]Levine, M. B., and Salama, M. A., "Mode Localization Experiments on a Ribbed Antenna," *Proceedings of the AIAA/ASME/ASCE/AHS/ASC 33rd Structures, Structural Dynamics, and Materials Conference*, AIAA, Washington, DC, 1992, pp. 2038–2047.

[18]King, M. E., and Vakakis, A. F., "Mode Localization in a System of Coupled Flexible Beams with Geometric Nonlinearities," *Zeitschrift für Angewandte Mathematik und Mechanik (ZAMM)* (to be published).

[19]Hodges, C. H., and Woodhouse, J., "Confinement of Vibration by One-Dimensional Disorder, I: Theory of Ensemble Averaging & II: A Numerical Experiment on Different Ensemble Averages," *Journal of Sound and Vibration*, Vol. 130, No. 2, 1989, pp. 237–268.

[20]Kissel, G. J., "Localization in Disordered Periodic Structures," Ph.D. Thesis, Massachusetts Inst. of Technology, Cambridge, MA, 1988.

[21]Pierre, C., "Weak and Strong Localization in Disordered Structures: A Statistical Investigation," *Journal of Sound and Vibration* (to be published).

[22]Photiadis, D. M., "Anderson Localization of One-Dimensional Wave Propagation on a Fluid-Loaded Plate," *Journal of the Acoustical Society of America*, Vol. 91, No. 2, 1992, pp. 771–780.

[23]Lust, S. D., Friedmann, P. P., and Bendiksen, O. O., "Free and Forced Response of Nearly Periodic Multi-Span Beams and Multi-Bay Trusses," *Proceedings of the AIAA/ASME/ASCE/AHS/ASC 32nd Structures, Structural Dynamics, and Materials Conference*, AIAA, Washington, DC, 1991, pp. 2831–2842.

[24]Nayfeh, A., and Mook, D., "Nonlinear Oscillations," Wiley, New York, 1984.

[25]Crespo Da Silva, M. R. M., and Zaretzky, C. L., "Non-Linear Modal Coupling in Planar and Non-Planar Responses of Inextensional Beams," *International Journal of Nonlinear Mechanics*, Vol. 25, No. 2, 1990, pp. 227–239.

[26]Crespo Da Silva, M. R. M., and Glynn, C. C., "Nonlinear Flexural-Torsional Dynamics of Inextensional Beams, I: Equations of Motion, & II: Forced Motions," *Journal of Structural Mechanics*, Vol. 6, No. 4, 1978, pp. 437–461.

[27]Pai, P.-J. F., "Nonlinear Flexural-Flexural-Torsional Dynamics of Metallic and Composite Beams," Ph.D. Thesis, Virginia Polytechnic Inst. and State Univ., Blacksburg, VA, 1992.

[28]Vakakis, A. F., and Rand, R. H., "Normal Modes and Global Dynamics of a Two Degree-of-Freedom Nonlinear System, I: Low Energies," *International Journal of Nonlinear Mechanics*, Vol. 27, No. 5, 1991, pp. 861–874.